Vol. 137: 23–31, 2019
https://doi.org/10.3354/dao03424

DISEASES OF AQUATIC ORGANISMS
Dis Aquat Org

Published online November 28

Pathologic findings and causes of death in southern right whales *Eubalaena australis*, Brazil

Kátia R. Groch[1,*], José L. Catão-Dias[1], Karina R. Groch[2], Cristiane K. M. Kolesnikovas[3], Pedro V. de Castilho[4], Luciana M. P. Moreira[5], Cecil R. M. B. Barros[5], Camila R. Morais de Medeiros[2], Eduardo P. Renault-Braga[2], Marcelo Sansone[6], Josué Díaz-Delgado[1]

[1]Laboratory of Wildlife Comparative Pathology, Department of Pathology, School of Veterinary Medicine and Animal Science, University of São Paulo, São Paulo, SP 05508-270, Brazil

[2]Instituto Australis/Projeto Baleia Franca, Imbituba, SC 88780-000, Brazil

[3]Associação R3 Animal, Rodovia João Gualberto Soares (SC-406), Barra da Lagoa, Florianópolis, SC 88061-500, Brazil

[4]Departamento de Engenharia de Pesca e Biologia (DEPB), Universidade do Estado de Santa Catarina, Bairro Progresso, Laguna, SC 88.790-000, Brazil

[5]Área de Proteção Ambiental da Baleia Franca/ICMBio, Imbituba, SC 88780-000, Brazil

[6]Instituto Adolfo Lutz, Centro de Patologia, Brasil, Pacaembú, São Paulo, SP 01246-000, Brazil

ABSTRACT: Southern right whales *Eubalaena australis* (SRWs) migrate to southern Brazil for breeding and calving from June through November. Overall, there is scarce knowledge on health status and pathologic conditions in SRWs. We report the pathologic and molecular investigation results of 8 SRWs that were necropsied between 2010 and 2017 within a breeding and calving ground in Santa Catarina state, Brazil. The animals were of various ages (7 newborns/calves, 1 adult) and sex (3 females, 5 males). Five whales stranded dead; 3 stranded alive and died shortly after (n = 2) or were euthanized (n = 1). The causes of stranding and/or death were neonatal respiratory distress syndrome with meconium aspiration (n = 3) with concomitant congenital hepatopathy in one of them; trauma of unknown origin (n = 3), infectious renal and lung disease with presumed sepsis (n = 1), and euthanasia (n = 1). Three animals were PCR-positive for cetacean morbillivirus; one of them also had morbilliviral antigen in kidney via immunohistochemical analysis. These results, integrating novel findings and a published report, contribute to the pathology knowledge of this species.

KEY WORDS: Cetacean · Fetal distress · Marine mammal · Meconium · Pathology · Southern right whale

1. INTRODUCTION

The southern right whale *Eubalaena australis* (hereafter SRW) is a migratory species that uses southern Brazilian waters as a nursery and breeding ground during austral winter and spring (Groch et al. 2005). In the Southwest Atlantic, intensive commercial whaling at the end of the 18th century drove a dramatic SRW population decline (Richards 2009). After the whaling ban in 1987, increasing numbers of right whales were sighted along with an increase in anthropogenic activities such as shipping and fishing (Groch et al. 2005). Overall, however, there is scarce knowledge on anthropogenic impacts and natural pathologic conditions in SRWs (Greig et al. 2001, Mouton et al. 2009, Reeb et al. 2010, Fiorito et al. 2015, 2016, McAloose et al. 2016, Bianchi et al. 2018, Groch 2018). Mortality rates for this species vary

*Corresponding author: katia.groch@gmail.com

widely among breeding grounds and years, and recent studies reported high numbers of deaths in Argentina (McAloose et al. 2016).

Herein, we report pathologic findings and molecular investigation results and correlate to cause of stranding and/or death (CSD) in 8 SRW that were necropsied between 2010 and 2017 in Santa Catarina state, Brazil.

2. MATERIALS AND METHODS

Between 2002 and 2017, a total of 27 SRWs stranded within the major breeding and calving ground off Santa Catarina state, Brazil (27° 25′ S, 48° 30′ W to 28° 42′ S, 49° 16′ W). We conducted necropsies and histopathologic analysis on 8 (29.6%) of the SRW carcasses. Epidemiological (stranding date, location) and biological data (status, age class, sex, total body length [TBL], body condition, and decomposition code; Geraci & Lounsbury 2005) were recorded. Age class was defined following McAloose et al. (2016) with major emphasis on TBL and degree of umbilical cord healing (patent, incomplete healing, healed). The body condition of each animal was classified as good, moderate, poor, or emaciated based on the degree of atrophy of the epaxial musculature, prominence of ribs, scapula or axial skeleton, and amount of subcutaneous, intrathoracic, and abdominal fat. Representative tissue samples of main organs (see Table S1 in the Supplement at www.int-res.com/articles/suppl/d137p023_supp.pdf) were collected and fixed in 10% neutral buffered formalin. The number and variety of necropsy samples varied among animals based on carcass condition and organ access. These tissues were trimmed, processed routinely for histology, and stained with hematoxylin and eosin (H&E). Liver sections of animal 6 were stained with Masson's trichrome (for collagen).

Real-time RT-PCR analysis for cetacean morbillivirus (CeMV) was performed in 5 animals. The methodology employed and partial results have been published in Groch et al. (2019). For immunohistochemical (IHC) analysis, we employed a monoclonal antibody against the nucleoprotein antigen of canine distemper virus (1:100; VMRD) known to cross-react with CeMV as described in Groch et al. (2019), and a polyclonal anti-myoglobin antibody (batch A324; 1:45000 dilution; Dako). For CeMV-IHC, lung from a CeMV-positive Guiana dolphin *Sotalia guianensis* and lung from a CeMV-negative Guiana dolphin were used as positive and negative tissue control, respectively. For myoglobin-IHC, positive control tissues included normal skeletal muscle (internal control) and non-human primate *Callithrix* sp. kidney with myoglobinuria (external control). As negative controls, primary antibodies were replaced by homologous non-immune serum. Antigen–antibody binding was detected by the Novolink Min Polymer Detection System (Leica Biosystems) and 'visualized' by use of 3, 3′ diaminobenzidine chromogen (Sigma D5637).

3. RESULTS

Of the 8 SRW carcasses examined in this study, 7 were newborns/calves; 6 of which had patent or incompletely healed umbilicus and 1 had a completely healed umbilicus. Three whales were female and 5 were male. Five whales stranded dead; 3 stranded alive and died shortly after (n = 2) or were euthanized (n = 1) (Table 1). Six of the 8 animals (75%) were in good body condition, whereas 2 (25%) were in poor body condition. Two animals were fresh (code 2), 4 were in moderate autolysis (code 3), and 2 had advanced autolysis (code 4) at necropsy. The most likely CSD (Table S1) were neonatal respiratory distress syndrome (NRDS) with meconium aspiration (animals 1, 6, and 8) and concomitant congenital hepatopathy (animal 6); trauma of unknown origin (animals 3, 4 and 5), euthanasia (animal 2; CeMV likely played a role in live-stranding), and infectious renal and lung disease with presumed sepsis (animal 7). A variety of gross and microscopic pathologic findings was observed in these animals (detailed in Table S1). Overall, trauma-associated lesions were prevalent in this cohort.

Animal 1 was a neonate male SRW that stranded alive and died shortly after (code 3 at necropsy). Grossly, a right corneal ulcer and marked bilateral conjunctival congestion were noted. The main microscopic finding was marked, diffuse atelectasia with abundant intra-alveolar and intrabronchiolar/bronchial squames and meconium. Additionally, the animal had diffuse splenic lymphoid depletion and acute monophasic segmental myodegeneration in skeletal muscle. IHC analysis revealed rare myoglobin-positive intratubular and tubuloepithelial intracytoplasmic globules in the kidney.

Animal 2 was an adult female SRW that stranded alive and remained beached for 7 d before euthanasia was performed (Kolesnikovas et al. 2012) due to poor prognosis. The animal developed severe cutaneous ulcers with marked necrosis of underlying soft tissues at pressure points. The carcass was code 3 at necropsy. Microscopically, the main findings were related to live-stranding including acute monophasic

Table 1. Stranding date, location coordinates, status (Al: alive; De: dead; [d]: died; [e]: euthanized), age class (Neo: neonate; Ad: adult; Ca: calf), sex (Ma: male; Fe: female), umbilicus state (Pa: patent; He: healed; IH: incompletely healed), total body length (TBL), body condition (BC), decomposition code (DC), cetacean morbillivirus (CeMV) results by immunohistochemistry (IHC) and real-time RT-PCR (tissues tested, positive in **bold**) and assumed cause of stranding and/or death (CSD) in southern right whales *Eubalaena australis*. ne: not examined

No.	Date	Coordinates	Status	Age	Umbilicus	Sex	TBL (m)	BC	DC	CeMV result		CSD
										IHC	RT-PCR	
1	9 Aug 2010	28° 26′ S, 48° 45′ W	Al [d]	Neo	Pa	Ma	5.28	Good	3	Negative	ne	Neonatal respiratory distress syndrome with meconium aspiration
2	7 Sep 2010	28° 21′ S, 48° 43′ W	Al [e]	Ad	He	Fe	13.94	Good	3	Positive (kidney)	**Kidney**, lung, liver, pancreas, mesenteric lymph node	Live-stranding stress response syndrome with multifocal compartment syndrome at pressure points; euthanized
3	17 Sep 2010	28° 42′ S, 49° 02′ W	De	Neo	Pa	Ma	4.3	Good	3	Negative	Lung	Trauma, unknown (also historical vessel collision and osseous deformities)
4	7 Aug 2011	28° 25′ S, 48° 44′ W	De	Ca	IH	Ma	5.5	Good	4	Negative	ne	Trauma, unknown
5	1 Aug 2012	28° 27′ S, 48° 45′ W	De	Neo	Pa	Ma	4.8	Poor	4	ne	ne	Trauma, unknown
6	21 Jul 2015	27° 54′ S, 48° 35′ W	De	Neo	IH	Fe	5.25	Good	3	Negative	Kidney, lung, liver, brain, mesenteric lymph node, spleen	Congenital hepatic fibrosis with cholestasis; neonatal respiratory distress syndrome with meconium aspiration and presumed water aspiration
7	1 Aug 2015	28° 07′ S, 48° 38′ W	De	Ca	He	Fe	5.4	Good	2	Negative	Kidney, **lung**, liver, spleen	Bacterial pyelonephritis (with presumed sepsis)
8	11 Aug 2017	28° 31′ S, 49° 10′ W	Al (d)	Neo	Pa	Ma	4.5	Poor	2	Negative	Kidney, **lung**, brain, prescapular lymph node, spleen	Neonatal respiratory distress syndrome with meconium aspiration

segmental myodegeneration in skeletal muscle and myocardium, acute passive hepatic congestion and scattered renal tubular proteinaceous and cellular casts that often labeled positive for myoglobin. Also, there was mild, multifocal, chronic renal interstitial fibrosis and rare tubular mineralization. PCR and IHC analyses for CeMV were positive in kidney tissue.

Animal 3 was a neonate male SRW that stranded dead (code 3 at necropsy). The animal presented partially healed propeller wounds on the left aspect of the peduncle (Fig. 1A), with mild fibrosis involving the underlying superficial musculature. These propeller-inflicted cutaneous incisions (craniocaudal decreasing length) involved a 90 cm long anterior section (regular edges, dorsoventral orientation, slight cranio-caudal tilt, approximately 90° angle with body axis); an 85 cm long middle section; and an 80 cm long caudal incision. These 3 main propeller cuts mildly reached the underlying superficial muscles. The interlaceration distance was 20–25 cm. There was no involvement of underlying or adjacent periosteal surfaces or bone structures. Additionally, the animal had multiple subcutaneous hematomas that extended longitudinally in the left cervicothoracic region (70 × 30 cm), in the right thoracic region (100 × 25 cm), and in the right peduncle (90 × 40 cm; Fig. 1B). Post-mortem examination of the defleshed and macerated skeleton revealed multiple osseous deformities involving the skull and cranial thoracic vertebral column (Fig. 2). These findings comprised marked left-lateral deviation of the longitudinal axis of the skull; deformation and ventromedial compression of the left supraoccipital, exoccipital, zygomatic process of squamosal and supraorbital process of the frontal bones; marked asymmetry of the alisphenoids (superior processes) and pterygoids (inferior processes); and unfused thoracic vertebral bodies and transverse processes with irregular and asymmetric laminae and left deviation of the neural arch to the left. Additionally, there was bilateral fusion of the first pair of cranial ribs, so called ‘bicipital ribs’ with an enlarged plate distally. Histopathologic analysis was precluded due to autolysis in this individual except for few well-preserved skin samples

Fig. 1. Macroscopic findings in a southern right whale *Eubalaena australis* (Case 3). (A) Focal propeller-inflicted partially healed cutaneous wound in the left dorso-lateral aspect of the peduncle. Inset: detail of partially healed propeller wound (longitudinal and perpendicular parallel wounds are indicated as dotted white and yellow lines). (B) focal subcutaneous hematoma

(collected immediately after carcass discovery), which revealed localized epidermal hyperplasia with keratinocyte degeneration, poikilocytes, and intracytoplasmic eosinophilic inclusion bodies (ICIBs) (Fig. 3).

Animal 4 was a male calf SRW stranded dead (code 4 at necropsy). The main gross finding was a 40 cm diameter subcutaneous hematoma in the left thoraco-abdominal region. Microscopically, there was

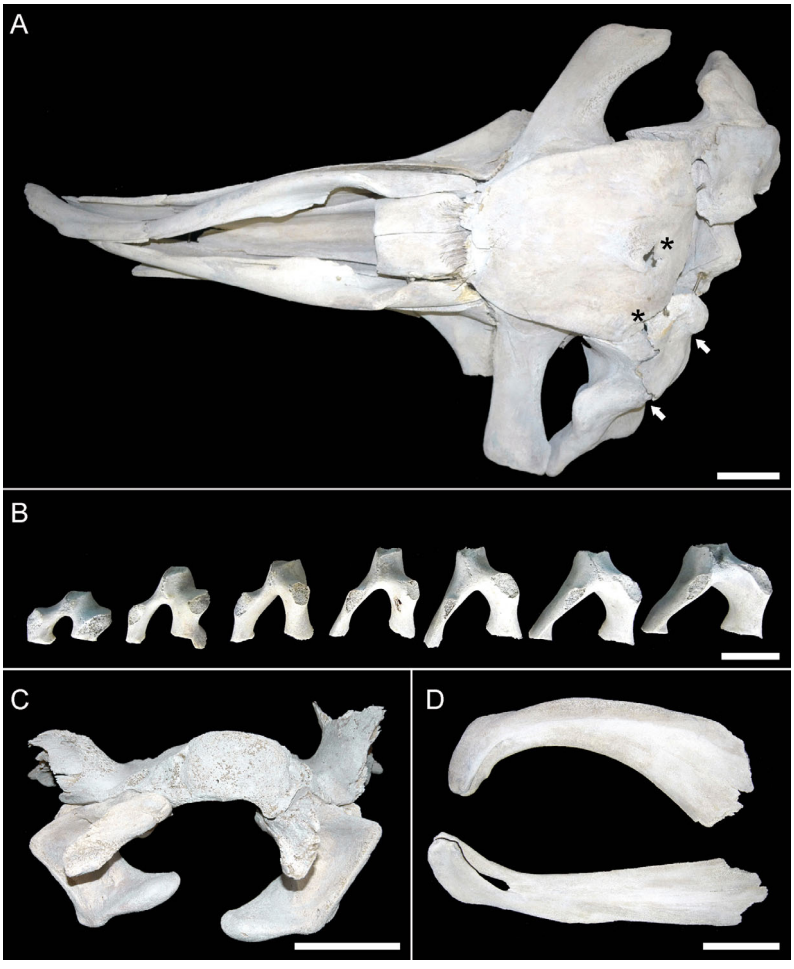

Fig. 2. Osseous deformities in a neonatal southern right whale *Eubalaena australis* (Case 3). (A) Dorsal view of the skull. There is remarkable left-lateral deviation of the longitudinal axis of the skull. The left portions of the supraoccipital and exoccipital bones as well as the zygomatic process of squamosal and supraorbital process of the frontal bone are deformed and compressed anteriorly (arrows). Two foci of bone rupture and loss are noted in the supraoccipital (asterisks). Extremities of maxilla and premaxilla are fractured and distorted due to artefact. Scale bar = 10 cm. (B) Anterior view of thoracic vertebra neural arches. The length and thickness of the lamina are asymmetric and the vertical axis is deviated to the left (right side of the image). The vertebral bodies and transverse processes were unfused and were removed in this picture. Scale bar = 5 cm. (C) Posterior view of the sphenoid bone. Marked asymmetry can be observed on alisphenoids (superior processes) and pterygoids (inferior processes). Scale bar = 5 cm. (D) Bilateral mid-distal fusion (note the enlarged plate distally) of the first and second ribs 'bicipital ribs' Scale bar = 10 cm

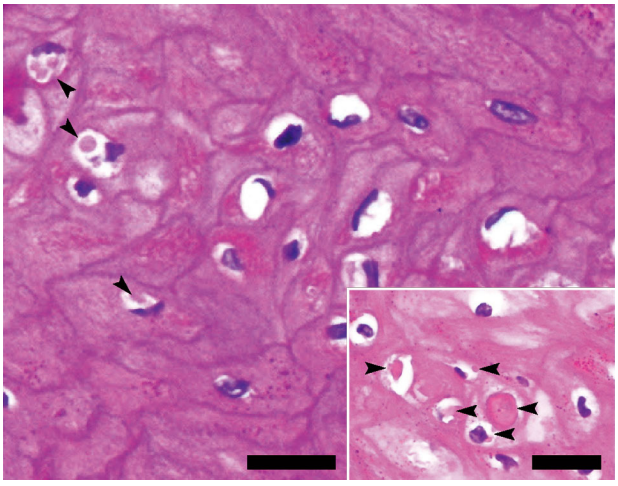

Fig. 3. Microscopic findings in southern right whales *Eubalaena australis*. Main image (Case 3): epidermis contains few swollen and poikilocytic keratinocytes with irregular eosinophilic intracytoplasmic inclusion bodies (ICIBs) compatible with poxvirus. Hematoxylin and eosin (H&E); scale bar = 50 µm. Inset (Case 5): similar ICIBs compatible with poxvirus in keratinocytes. H&E; scale bar = 50 µm

acute monophasic segmental myodegeneration in the skeletal muscle.

Animal 5 was a neonate male SRW stranded dead (code 4 at necropsy). Grossly, there were multifocal subcutaneous hematomas ranging from 20–55 cm in diameter throughout the right cephalic, cervical, thoracic, and abdominal regions along with hemothorax. Microscopically, the whale had localized epidermal hyperplasia with keratinocyte degeneration, poikilocytes, and ICIBs (Inset in Fig. 3).

Animal 6 was a neonate female SRW stranded dead (code 3 at necropsy). The main gross findings were marked pulmonary edema and generalized icterus (Fig. 4A). Microscopically, there was marked, diffuse atelectasia with abundant aspirated squames, fibrin, edema, and histiocytic alveolitis with multinucleated giant cells (Fig. 4B). In the liver, there was marked, multifocal, chronic periportal bridging fibrosis with lobular distortion and collapse, bile duct hyperplasia, hepatocyte atrophy and loss, and marked cholestasis (Hall's-positive) (Fig. 4C) with necrosis. Furthermore, this animal had acute renal tubular degeneration and scattered Hall's-negative and myoglobin-positive intratubular casts (Fig. 4D) identical to those observed in animals 1 and 2.

Animal 7 was a female calf SRW stranded dead (code 2 at necropsy). Grossly, the whale had bilateral 20 cm in diameter cephalic cutaneous hematomas and generalized cutaneous cyamidiasis. Microscopically, there was marked, multifocal, acute suppurative and necrotizing pyelonephritis (Fig. 5) with hemorrhage, intratubular bacteria and focal thrombosis along with a generalized increase in circulating leukocytes, primarily neutrophils and macrophages, suggesting sepsis. In the lung, there was diffuse edema and multifocal interstitial pneumonia. PCR analysis from lung tissue was positive for CeMV.

Animal 8 was a neonate male SRW that stranded alive and died shortly after (code 2 at necropsy). The main microscopic findings were marked, diffuse atelectasia with abundant intra-alveolar and intrabronchiolar/bronchial squames and meconium; multicentric lymphoid depletion (mediastinal lymph node, spleen); diffuse brain congestion with scattered acute hemorrhage, and mild lymphocytic meningitis with hemorrhage in cerebral cortex and choroid plexus of the fourth ventricle. PCR analysis from lung tissue was positive for CeMV.

Phylogenic analysis based on the sequenced amplicons from animals 2 and 7 showed the samples shared 99.5% nucleotide and 98.5% amino acid identity with the Guiana dolphin CeMV sequence (Groch et al. 2019). Kidney from animal 2 had positive immunolabeling in the cytoplasm of epithelium of proximal convoluted tubules and intratubular casts (Groch et al. 2019).

4. DISCUSSION

Herein, we report the pathologic results in a cohort of SRWs stranded in Santa Catarina state, southern Brazil, between 2010 and 2017. The small cohort of whales evaluated here did not correspond to any identifiable period of increased mortality rate of this species (Thomas et al. 2013, McAloose et al. 2016). Neonates/calves were overrepresented in the sample set, as expected in a calving ground (McAloose et al. 2016, Groch et al. 2018). Parallel TBL and degree of umbilical cord healing examination allowed distinction between newborn/neonates and young calves. In 2 cases (animals 1 and 4), the umbilical cord was not completely healed even though TBL was slightly greater than 5.0 m. This is in slight contrast with McAloose et al. (2016), where all neonatal SRW with healed umbilici had TBL below 5.0 m. However, given the reduced sample size in the present study, no further conclusions can be drawn other than TBL at birth vs. degree of umbilical closure is likely to present variations.

Pathologic postmortem investigations allowed determination of most likely CSD in all animals except for animal 2. A common CSD in 3 animals was based

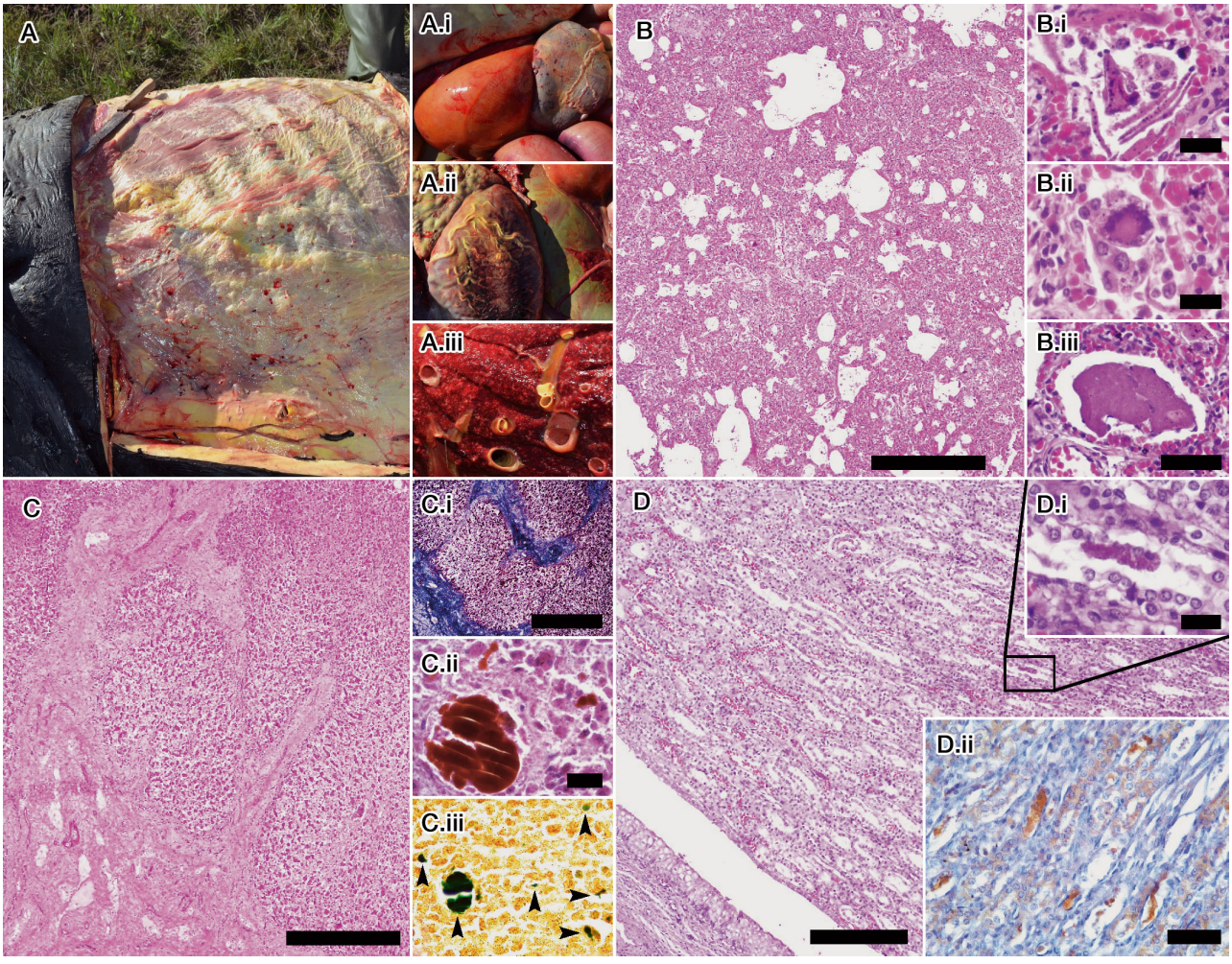

Fig. 4. Gross and microscopic findings in a southern right whale *Eubalaena australis* (Case 6). (A) The subcutaneous fat and fasciae are icteric, as are (A.i) stomach and splenic capsule, (A.ii) heart and Glisson's capsule of liver, and (A.iii) intrapulmonary vascular walls. (B) Diffusely, the alveoli are collapsed and hypercellular. Hematoxylin and eosin (H&E); scale bar = 500 µm. Insets: (B.i) few keratin squames along with reactive and foamy histiocytes within an alveolus. H&E; scale bar = 50 µm. (B.ii) Focally, intraalveolar histiocytic inflammation also includes multinucleate giant cells. H&E; scale bar = 50 µm. (B.iii) focal intra-alveolar fibrin. H&E; scale bar = 100 µm. (C) The hepatic parenchyma is markedly distorted having periportal bridging fibrosis with lobular collapse and loss. H&E; scale bar = 500 µm. Insets: (C.i) Abundant collagen (blue) in fibrotic portal triads and disrupted terminal plates. Masson's trichrome; scale bar = 500 µm. (C.ii) there are intracanalicular and intraductular bile plugs. H&E; scale bar = 100 µm. (C.iii) Bile plugs (arrowheads) stain green by Hall's histochemical technique. Scale bar = 50 µm. (D) Low-power detail of renicular medulla with scattered intratubular proteinaceous plugs (black box). H&E; scale bar = 200 µm. Insets: (D.i) detail of proteinaceous plug in main figure. H&E; scale bar = 50 µm. (D.ii) Myoglobin-positive intratubular plugs and tubuloepithelial cytoplasmic labeling. IHC for myoglobin; scale bar = 100 µm

on gross evidence of trauma of undetermined etiology. Animal 3 had evidence of historical vessel collision exemplified by partially healed propeller cuts in the peduncle. This animal had multifocal severe osseous deformities involving multiple axial skeletal segments. The etiology of these findings was not readily evident, and 2 main explanations were given consideration: trauma and congenital skeletal dysplasia. The former was given consideration based on ipsilaterality to propeller's cut and rather localized osseous involvement distribution including the skull and cranial thoracic vertebrae. Also, 2 focal areas of bone fracture/osteolysis were noted in the left supraoccipital bone and there was considerable ventromedial distortion of the left supraoccipital, exoccipital, basioccipital, and basisphenoid bones and associated apophyses. No evident calluses were observed in these bones; however, their absence could be hypothetically related to the nature of the trauma at this anatomic location and chondro-osseous immaturity

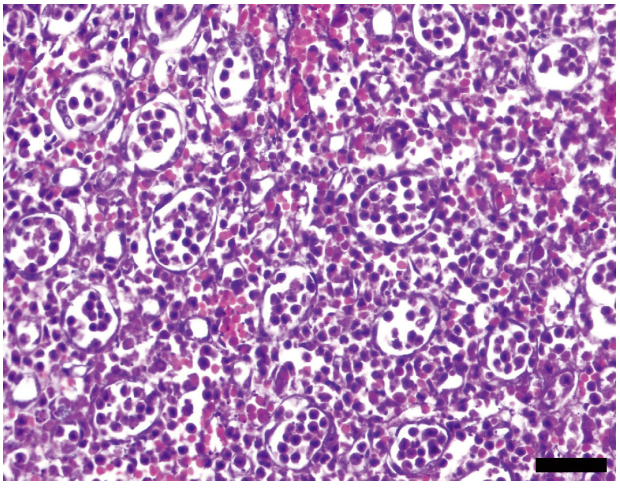

Fig. 5. Microscopic findings in southern right whale *Eubalaena australis* (Case 7). The renal distal convoluted tubules and Henle's loops are infiltrated and disrupted by abundant neutrophils that extend into the interstitium. Hematoxylin and eosin (H&E); scale bar = 50 µm

at this level. The incidence of skeletal dysplasias or osseous congenital anomalies in cetaceans is unknown for most species, yet it seems to be high in the Peale's dolphin *Lagenorhynchus australis* (San Martín et al. 2016). Reported congenital bone anomalies in cetaceans may include vertebral defects, e.g. cervical ribs, unfused neural arch, fused neural spinous processes, spina bifida, kyphosis, lordosis, scoliosis, as well as conjoined twins, rudimentary hind limbs and digital anomalies such as polydactyly and polyphalangy (Cooper & Dawson 2009, Groch et al. 2012, San Martín et al. 2016). For a succinct review see Colegrove (2018). In the present case, to the best of our knowledge the cephalic osseous anomalies have no evident counterpart in the medical literature. Furthermore, the alterations in the first pair of ribs were compatible with rib fusion (Groch et al. 2012). Additionally, this whale had multiple subcutaneous hematomas. The etiology of the hematomas was likely trauma and although ship collision was given consideration, the relatively 'fresh' appearance and multifocal distribution of these hematomas precluded ruling out traumatic intra- or interspecific interactions (Groch et al. 2018, Díaz-Delgado et al. 2018). While some studies have documented the chronology of skin wound healing in certain cetacean species (Bruceallen & Geraci 1985, Geraci & Bruceallen 1987, Krutzen et al. 2002, Giménez et al. 2011), there is no available information on hematoma progression and resolution in these species. In contrast to animal 3, animals 4 and 5 had subcutaneous hematomas that suggested more severe, as per greater extension, localized (animal 4) and multiple but ipsilateral (animal 5) trauma. These were more suggestive of vessel collision (Groch et al. 2018).

NRDS is increasingly being recognized in cetaceans (Díaz-Delgado et al. 2018). In this condition, lungs typically have diffuse bilateral edema, and microscopically, the alveoli and distal airways are filled with proteinaceous (hypereosinophilic) fluid along with squames and often meconium particles. These findings were readily evident in 3 neonates/calves (with incompletely healed umbilici); the severity and extent of the lesions could explain stranding and/or death in these whales. The underlying pathogenesis in these cases, including potential dystocia, is unknown; however, animal 6 had severe underlying hepatopathy and animal 8 was positive for CeMV by PCR in lung tissue (Groch et al. 2019). McAloose et al. (2016) found molecular evidence of *Brucella* spp. in lung tissue of a newborn/neonatal SRW calf with interstitial pneumonia and aspirated squames; however, IHC results were negative. A causal link could not be entirely confirmed or discarded. We did not investigate *Brucella* in the present study so we cannot rule out this pathogen.

Animal 6 had marked, multifocal, chronic periportal bridging fibrosis with lobular distortion and collapse, mild bile duct hyperplasia, mild portal vein hypoplasia, hepatocyte atrophy, and loss and marked cholestasis with necrosis. Overall, these findings are not specific and may be present in a number of congenital and acquired diseases involving the hepatic parenchyma and biliary tree (Cullen & Stalker 2016). As this animal was a neonate, these findings were best interpreted as a congenital (born with) fibrosing hepatopathy. However, the true nature of the above findings remains obscure. A condition coined 'congenital hepatic fibrosis' (CHF) is often described in humans (Desmet 1992) and dogs (Cullen & Stalker 2016) and was given consideration in this case. However, findings that often accompany CHF (e.g. polycystic kidneys, compensatory arteriolar proliferation) were not evident in this case. Severe cholestasis with generalized icterus was a striking feature in this case, yet it is uncommon in CHF (Desmet 1992, Cullen & Stalker 2016). Other congenital hepatobiliary anomalies (developmental disorders), acquired infectious or non-infectious disease processes were deemed less likely based on histomorphological examination (Cullen & Stalker 2016). Autolysis limited further analysis. To our knowledge, this is a novel hepatobiliary finding in marine mammals.

Animal 2, an adult lactating SRW, stranded alive and was euthanized 7 d later (Kolesnikovas et al.

2012). Prolonged sternal decubitus led to severe pressure ulcers recapitulating pathologic features of compartment-like syndrome (Cooper & Valentine 2016). 'Stranding stress response' likely played a major aggravating role in this case, further supported by microscopic muscle and liver findings. However, no confirmatory biochemical data were available. This animal had morbilliviral genetic material and IHC evidence of viral replication (as suggested by nucleoprotein detection) in the kidney. Although the etiopathogenic role of CeMV in this case remains unknown, CeMV could have played a role in live stranding. Lung tissue of 2 calves (animals 7 and 8) was positive for CeMV by PCR (Groch et al. 2019). Only the former had multifocal interstitial pneumonia, but the lack of characteristic morbilliviral intranuclear and intracytoplasmic inclusion bodies and viral antigen precluded definitive direct pathogen–lesion confirmation. Also, this animal had suppurative bacterial pyelonephritis and systemic leukocytosis, suggesting sepsis. A potential association with pneumonia could not be ruled out in this case. Unfortunately, no bacterial culture was performed. Animal 8 had focal lymphocytic meningitis and choroid plexitis of the fourth ventricle; and CeMV PCR analysis of brain tissue was negative. Similar meningeal inflammation was noted in various SRW neonates/calves (McAloose et al. 2016); however, as in those cases the etiology in the present case is unknown. We surmise these cases may represent vertical *in utero* transmission, and although the chronology of infection is not known, recent infection and/or compromised immunologic response could explain these findings (Groch et al. 2019). Further research is warranted. CeMV investigation should be included in health assessments of SRWs.

Other interesting findings in this study included poxviral dermatopathy in 2 whales with microscopic findings identical to those reported in Argentinean SRWs (Fiorito et al. 2015). Also, generalized cutaneous cyamidiasis was observed in a calf infected by CeMV (animal 7), in agreement with reports linking CeMV infection and overt ectoparasitosis/epibiosis (Aznar et al. 2005) as well as non-specific generalized ill health (Pettis et al. 2004). We did not observe gross lesions compatible with kelp gull–whale interactions in these whales (Thomas et al. 2013, McAloose et al. 2016).

In conclusion, our results provide evidence of natural (non-anthropogenic) disease processes and anthropogenic threats in SRW. Natural CSD included neonatal respiratory distress syndrome with meconium aspiration, and infectious renal and lung disease with presumed sepsis. PCR and/or IHC evidence of CeMV was observed in 1 adult and 2 calves; its etiopathogenic role and potential conservation implication remain unknown in this species. Other CSD included trauma of unknown origin. These results, integrating novel findings and a published report, contribute to pathology knowledge on this species.

Acknowledgements. We acknowledge numerous people for their assistance in stranding monitoring and necropsy procedures: volunteers and staff members of Instituto Australis/ Projeto Baleia Franca, Área de Proteção Ambiental da Baleia Franca/ ICMBio, Centro Mamíferos Aquáticos/ICMBio, Associação R3 Animal, Unidade de Zoologia 'Profª Morgana Cirimbelli Gaidzinski' – MUESC/UNESC–Criciúma, Laboratório de Zoologia/UDESC. Thanks to the 'Protocolo de Encalhes da APA da Baleia Franca' (local marine mammal stranding network since 2010), Southern Marine Mammal Stranding and Information Network (REMASUL), the National Network (REMAB), CMA/ICMBio, Andrade Gutierrez, Santos Brasil, Exército Brasileiro (Brazilian Army), Environmental Police of Santa Catarina State, and Capitania dos Portos-Delegacia de Laguna (Brazilian Navy) for their help and support in the case of the whale stranded alive in 2010. Laguna and Imbituba City Halls helped with equipment during necropsies. Special thanks to Neiva T. Spinato for much valuable technical assistance in several stranding events and especially for skeletal reconstruction of specimens. This research was also supported by Coordination for the Improvement of Higher Education Personnel (CAPES) and São Paulo Research Foundation (FAPESP), grants #2014/24932-2; #2015/00735-6; and #2017/02223-8. J.L.C.D. is the recipient of a fellowship from the National Research Council (CNPq; grant # 305349/2015-5).

LITERATURE CITED

Aznar FJ, Perdiguero D, Pérez del Olmo A, Repullés A, Agustí C, Raga JA (2005) Changes in epizoic crustacean infestations during cetacean die-offs: the mass mortality of Mediterranean striped dolphins *Stenella coeruleoalba* revisited. Dis Aquat Org 67:239–247

Bianchi MV, Ehlers LP, Vargas TP, Lopes BC and others (2018) Omphalitis, urachocystitis and septicemia by *Streptococcus dysgalactiae* in a southern right whale calf *Eubalaena australis*, Brazil. Dis Aquat Org 131: 227–232

Bruceallen LJ, Geraci JR (1985) Wound-healing in the bottlenose dolphin (*Tursiops truncatus*). Can J Fish Aquat Sci 42:216–228

Colegrove KM (2018) Noninfectious diseases. In: Gulland FM, Dierauf LA, Whitman KL (eds) CRC handbook of marine mammal medicine. CRC Press, Boca Raton, FL, p 267–296

Cooper LN, Dawson SD (2009) The trouble with flippers: a report on the prevalence of digital anomalies in Cetacea. Zool J Linn Soc 155:722–735

Cooper BJ, Valentine BA (2016) Muscle and tendon. In: Maxie MG (ed) Jubb, Kennedy, and Palmer's pathology of domestic animals, Vol 1. Elsevier, St. Louis, MO, p 164–249

Cullen JM, Stalker MJ (2016) Liver and biliary system. In: Maxie MG (ed) Jubb, Kennedy, and Palmer's pathology of domestic animals, Vol 2. Elsevier, St. Louis, MO, p 258–352

Desmet VJ (1992) What is congenital hepatic fibrosis? Histopathology 20:465–477

Díaz-Delgado J, Fernandez A, Sierra E, Sacchini S and others (2018) Pathologic findings and causes of death of stranded cetaceans in the Canary Islands (2006-2012). PLOS ONE 13:e0204444

Fiorito C, Palacios C, Golemba M, Bratanich A and others (2015) Identification, molecular and phylogenetic analysis of poxvirus in skin lesions of southern right whale. Dis Aquat Org 116:157–163

Fiorito CD, Bentancor A, Lombardo D, Bertellotti M (2016) *Erysipelothrix rhusiopathiae* isolated from gull-inflicted wounds in southern right whale calves. Dis Aquat Org 121:67–73

Geraci JR, Bruceallen LJ (1987) Slow process of wound repair in beluga whales, *Delphinapterus leucas*. Can J Fish Aquat Sci 44:1661–1665

Geraci JR, Lounsbury VJ (2005) Marine mammals ashore: a field guide for strandings. National Aquarium in Baltimore, Baltimore, MD

Giménez J, De Stephanis R, Gauffier P, Esteban R, Verborgh P (2011) Biopsy wound healing in long-finned pilot whales (*Globicephala melas*). Vet Rec 168:101

Greig AB, Secchi ER, Zerbini AN, Rosa LD (2001) Stranding events of southern right whales, *Eubalaena australis*, in southern Brazil. J Cetacean Res Manag 2:157–160

Groch KR (2018) Conservation advances for the southern right whales in Brazil. In: Rossi-Santos MR, Finkl CW (eds) Advances in marine vertebrate research in Latin America: technological innovation and conservation. Springer Nature, Cham

Groch KR, Palazzo JT Jr, Flores PAC, Adler FR, Fabian ME (2005) Recent rapid increases in the Brazilian right whale population. Lat Am J Aquat Res 4:41–47

Groch KR, Marcondes MC, Colosio AC, Catão-Dias JL (2012) Skeletal abnormalities in humpback whales *Megaptera novaeangliae* stranded in the Brazilian breeding ground. Dis Aquat Org 101:145–158

Groch KR, Diaz-Delgado J, Marcondes MCC, Colosio AC and others (2018) Pathology and causes of death in stranded humpback whales (*Megaptera novaeangliae*) from Brazil. PLOS ONE 13:e0194872

Groch KR, Groch KR, Kolesnikovas CK, de Castilho PV and others (2019) *Cetacean morbillivirus* in southern right whales, Brazil. Transbound Emerg Dis 66:606–610

Kolesnikovas CK, Groch KR, Groch KR, De Moraes AN and others (2012) Euthanasia of an adult southern right whale (*Eubalaena australis*) in Brazil. Aquat Mamm 38: 317–321

Krutzen M, Barre LM, Moller LM, Heithaus MR, Simms C, Sherwin WB (2002) A biopsy system for small cetaceans: darting success and wound healing in *Tursiops* spp. Mar Mamm Sci 18:863–878

McAloose D, Rago MV, Di Martino M, Chirife A and others (2016) Post-mortem findings in southern right whales *Eubalaena australis* at Peninsula Valdes, Argentina, 2003–2012. Dis Aquat Org 119:17–36

Mouton M, Reeb D, Botha A, Best P (2009) Yeast infection in a beached southern right whale (*Eubalaena australis*) neonate. J Wildl Dis 45:692–699

Pettis HM, Rolland RM, Hamilton PK, Brault S, Knowlton AR, Kraus SD (2004) Visual health assessment of North Atlantic right whales (*Eubalaena glacialis*) using photographs. Can J Zool 82:8–19

Reeb D, Best PB, Botha A, Cloete KJ, Thornton M, Mouton M (2010) Fungi associated with the skin of a southern right whale (*Eubalaena australis*) from South Africa. Mycology 1:155–162

Richards R (2009) Past and present distributions of southern right whales (*Eubalaena australis*). NZ J Zool 36: 447–459

San Martín AA, Macnie SV, Goodall RNP, Boy CC (2016) Pathology in skeletons of Peale's dolphin *Lagenorhynchus australis* from southern South America. Dis Aquat Org 120:9–15

Thomas P, Uhart M, McAloose D, Sironi M and others (2013) Workshop on the southern right whale die-off at Península Valdés, Argentina. Document SC/65/BRG15. International Whaling Commission Scientific Committee meeting, 3–15 June 2013, Jeju

Editorial responsibility: Michael Moore, Woods Hole, Massachusetts, USA

Submitted: December 12, 2018; Accepted: September 6, 2019
Proofs received from author(s): November 21, 2019